Mast cells as immune regulators in atherosclerosis

Kritikou, E.

Chapter 3

Inhibition of lysophosphatidic acid receptors 1 and 3 attenuates atherosclerosis development in LDL-receptor deficient mice

Sci Rep. 2016; 6:37585

[1]Eva Kritikou
[1]Gijs H.M. van Puijvelde
[1]Thomas van der Heijden
[1]Peter J. van Santbrink
[1]Maarten Swart
[1]Frank H. Schaftenaar
[1]Mara J. Kröner
[1]Johan Kuiper
[1]Ilze Bot

[1] Division of Biopharmaceutics, Leiden Academic Centre for Drug Research, Leiden University, Leiden, The Netherlands

Abstract

Lysophosphatidic acid (LPA) is a natural lysophospholipid present at high concentrations within lipid-rich atherosclerotic plaques. Upon local accumulation in the damaged vessels, LPA can act as a potent activator for various types of immune cells, through its specific membrane receptors $LPA_{1/3}$. LPA elicits chemotactic, pro-inflammatory and apoptotic effects that lead to atherosclerotic plaque progression. In this study we aimed to inhibit LPA signaling by means of $LPA_{1/3}$ antagonism using the small molecule Ki16425. We show that $LPA_{1/3}$ inhibition significantly impaired atherosclerosis progression. Treatment with Ki16425 also resulted in reduced CCL2 production and secretion, which led to less monocytes and neutrophil infiltration. Furthermore, we provide evidence that $LPA_{1/3}$ blockade enhanced the percentage of non-inflammatory, $Ly6C^{low}$ monocytes and $CD4^{+}CD25^{+}FoxP3^{+}$ T regulatory cells. Finally, we demonstrate that $LPA_{1/3}$ antagonism mildly reduced plasma LDL cholesterol levels. Therefore, pharmacological inhibition of $LPA_{1/3}$ receptors may prove a promising approach to diminish atherosclerosis development.

1. Introduction

Atherosclerosis is a lipid-driven chronic inflammatory syndrome, accountable for the majority of acute cardiac episodes and comprising, at present, a principal cause of death in Western societies[1]. The disorder initiates upon damage of the arterial endothelium, induced by high shear stress and excessive amounts of cholesterol in the form of low-density lipoproteins (LDL). LDL can accumulate within the subendothelial space, triggering the immune system to launch an inflammatory cascade[2,3]. Thereupon, circulating monocytes infiltrate and ingest modified LDL particles, differentiating into macrophage foam cells; the main components of an atherosclerotic plaque. An additional influx of pro-atherogenic innate cells, such as neutrophils[4] and mast cells[5], follows, along with the rise of specific adaptive immune responses through presentation of lipid antigens by antigen presenting cells[6]. This process results in the infiltration of various subtypes of T cells, the main one being $CD4^+$ T helper 1 (T_{H1}) cells[7-9]. Evidently, an uncontrollable increase in the atherosclerotic plaque size, or rupture of the plaque, may lead to life-threatening clinical events.

Lysophosphatidic acid (LPA) is a bioactive glycerophospholipid found elevated in the circulation of patients with acute coronary syndromes[8], and directly linked to hyperlipidemia[9,10]. The presence of LPA in the serum has been mainly associated with platelet activation[11], but has also been described inside human atherosclerotic specimens[12], as well as in the plaques of $LDLr^{-/-}$ mice, with an increasing concentration rate upon disease progression[13]. Intraplaque LPA is enzymatically formed *in situ,* upon mild modification of the LDL molecule[14] and elicits its effects *via* 9 different G-protein coupled receptors ($LPA_{1\text{-}6,}$ GPR87, P2Y10 and GPR35) which have been classified into different subcategories based on their structural diversity and ligand specificity[15,16]. Of these receptors, LPA_1, LPA_2 and LPA_3 are structurally similar and belong to the Endothelial Differentiation Gene (EDG) family of proteins[17], with their general mode of action leading to gene regulation, chemokine secretion and cell survival[18]. Interestingly, LPA can activate mast cells[19,20] and neutrophils[21], as well as influence the migration of $CD4^+$ T helper cells[22]; all key cell types that are directly implicated in atherosclerosis. The impact of LPA on atherosclerosis has been thoroughly studied in the past, and reviewed in detail by Schober & Siess[23], with its role extending from increased infiltration and activation of monocytes to enhanced foam cell formation and elevated levels of endothelial permeability. Specifically, the chemotactic effects induced through LPA are linked to upregulation of inflammatory chemokines and adhesion molecules such as CCL2[24], CXCL1[25] and I-CAM 1[26]. The pro-atherosclerotic effects of LPA have been mainly tied to LPA_1 and $LPA_{3,}$ which were reported to increase atherosclerosis development in $apoE^{-/-}$ mice[27]. Receptors LPA_1 and LPA_3 are widely expressed by immune cells[28,29], as well as endothelial[30] and vascular smooth muscle cells[31], with LPA_3 activation being

involved in cell migration[32], while LPA_1 shows both migratory[33] and apoptotic effects[34].

In this study, we aimed to examine the development of atherosclerosis upon pharmacological blockade of receptors LPA_1 and LPA_3 ($LPA_{1/3}$), using the synthetic antagonistic compound Ki16425[35].

2. Materials & Methods

2.1 Animals

$LDLr^{-/-}$ mice were initially obtained from the Jackson Laboratories and bred at the Leiden University animal facility, with water and food supply *ad libitum*. All animal work was approved by the Leiden University Animal Ethics committee and performed according to the guidelines established by the Dutch government and European Union.

2.2 Atherosclerosis

Atherosclerosis was induced in male $LDLr^{-/-}$ mice (10-11 weeks old) by feeding a Western type diet (WTD) (0.25% cholesterol, 15% cocoa butter; Special Diet Services, Essex, UK) for 2 weeks prior and throughout the course of the treatment. Subsequently, 12-15 mice per group were randomized based on age, weight and/or cholesterol levels and injected intraperitoneally 3 times a week with either a vehicle control or 5mg/kg of the $LPA_{1/3}$ antagonist, Ki16425; the injections were performed for 6 weeks. All mice were monitored for body weight changes every week throughout the treatment period; at the experimental endpoint, weight was additionally determined in organs such as the spleen and liver.

2.3 Immunohistochemistry

The mice were anaesthetized with a mix of ketamine (100mg/ml), sedazine (25mg/ml) and atropine (0.5mg/ml) and perfused with PBS through heart puncture in the ventricles. The hearts were dissected below the atria and sectioned perpendicularly to the axis of the aorta, starting within the heart and in the direction towards the aortic arch. Upon aortic root identification by the appearance of the aortic valve leaflets, 10μm sections were collected and mounted on gelatin-coated slides. Mean plaque area (in μm^2) was calculated for six sequential Oil-Red-O stained sections in distal direction, starting at the point where all three aortic valve leaflets first appeared. Plaque macrophages were stained using a MOMA-2 antibody at a 1:1000 concentration (rat IgG2b, Serotec Ltd.). For the MOMA-2 levels in the plaques, three subsequent sections displaying the highest plaque content per mouse were analyzed. Mast cells and neutrophils were visualized by staining with a Naphthol AS-D chloro-acetate esterase kit (Sigma Aldrich) and counted manually. A mast cell was considered resting when all granules were maintained inside the cell, while mast cells were assessed as activated when granules were deposited in the tissue surrounding the mast cell. Neutrophils were identified as round cells with a characteristic lobular nucleus and pink granular cytoplasm. T cell numbers were determined following a CD3 staining at a 1:150 concentration (clone S7P, ThermoScientific). All microscopic analyses were performed on a Leica DM-RE microscope and ORO, as well as MOMA-2, quantifications were carried out using Leica QWin software (Leica, Imaging Systems, UK) and through blinded independent analysis.

2.4 RT-PCR

Isolation of mRNA was performed on the liver and aortic arch of 8 mice/group, based on the guanidium isothiocyanate method[58]. Subsequently, the M-MuLV reverse transcriptase (RevertAid, Leon-Roth) was used for the reverse transcription. The quantitative analysis of specific gene expression was executed on a 7500 Fast-real time PCR system (Applied Biosystems, Foster City, CA) using SYBR Green Technology. The relative expression was determined based on two housekeeping genes; β-actin and ribosomal protein L27 (Rpl27). The complete primer list is included in the **Supplementary Table S1**.

2.5 Serum analysis

Throughout the study, tail blood was collected by a tail-vein cut; serum was obtained by centrifugation at 8.000 rpm for 10 minutes. Total cholesterol levels in the serum were measured at week 0, 3 and 6 of the treatment by an enzymatic colorimetric assay and in comparison to an internal Precipath control (standard serum provided by Roche Diagnostics). At the end of the experiment, cholesterol fraction separation for lipoprotein particle analysis was obtained after processing 30μL serum/mouse through a Superose 6 column (Smart System, Pharmacia). Subsequent measurement of cholesterol levels in the retrieved fractions was performed as described above. CCL2 levels in the serum of 13 mice/group were analyzed by ELISA (BD Biosciences) according to the manufacturer's protocol.

2.6 Flow cytometry

Blood was collected as described above; Red blood cells were lysed using an erythrocyte lysis buffer (0.1mM EDTA, 10mM $NaHCO_3$, 1mM NH_4Cl, pH=7.2). Subsequently, white blood cells were stained with the relevant antibodies for flow cytometry analysis (**Supplementary Table S2**). Spleen tissue was harvested from all mice and processed through a 70μm cell strainer to acquire single cell suspensions. Subsequently, cells underwent lysis once, for erythrocyte disposal, and were stained for flow cytometry. In approximation, 200.000 cells per sample were stained with antibodies against extracellular proteins at a concentration of 0.1 μg/sample for 30 minutes. For the detection of intracellular antibodies all cells were fixated, permeabilized using the transcription factor kit (Ebioscience) and stained at a concentration of 0.3 μg/sample. All flow cytometry experiments were executed on a FACS Canto II and data were analyzed using FlowJo software.

2.7 Statistics

All data are analyzed using the GraphPad Prism software and presented as mean±SEM. A 2-tailed Student's *t*-test was used to compare individual groups. Non-Gaussian distributed data were analyzed using a 2-tailed Mann-Whitney *U* test. For the analysis of two or more variables a two-way ANOVA was used with the Bonferroni post-test for multiple comparisons. The probability (alpha) for all tests was set to 0.05 with values lower than this considered significant ($P<0.05$).

3. Results

3.1 $LPA_{1/3}$ inhibition reduces atherosclerotic plaque size

To assess the effect of $LPA_{1/3}$ inhibition on atherosclerosis, $LDLr^{-/-}$ mice were injected intraperitoneally with either Ki16425 (5mg/kg) or a vehicle-control for 6 weeks,

(3x/week). Plaque size quantification, using an Oil-Red-O staining showed that mice treated with the $LPA_{1/3}$ inhibitor had significantly smaller plaque size (-40%) compared to control mice (**Figure 1A**, Ki16425: $89*10^3 \pm 9*10^3$ µm² vs control: $147*10^3 \pm 21*10^3$ µm², P=0.023). In fact, plaque size was significantly lower in the treated group at each distance measured from the start of the three-valve area up to its end (**Figure 1B**). A MOMA-2 staining was performed to evaluate the intra-plaque macrophage levels. The absolute macrophage content of the Ki16425 treated group was significantly lower (-45%) compared to the control (**Figure 1C**, Ki16425: $36*10^3 \pm 8*10^3$ µm² vs control: $65*10^3 \pm 6*10^3$ µm², P=0.006), whereas the relative amount (% macrophage levels of the plaque) was not significantly different (**Figure 1D**, P=0.11). Furthermore, the aortic root area was analyzed for mast cell and neutrophil content, since both immune cell types express $LPA_{1/3}$ and are involved in atherosclerosis progression. No differences in the number or activation status of mast cells were detected between the two groups (**Figure 1E**, P=0.38 for mast cell # and Fig.1F, P=0.88 for activated mast cell #). However, a substantial reduction in the number of infiltrated neutrophils (-31%) upon $LPA_{1/3}$ blockade was observed (**Figure 1G**, Ki16425:8.5±0.7 neutrophils/µm² tissue vs. control: 12.4±0.9 neutrophils/µm² tissue, P=0.004).

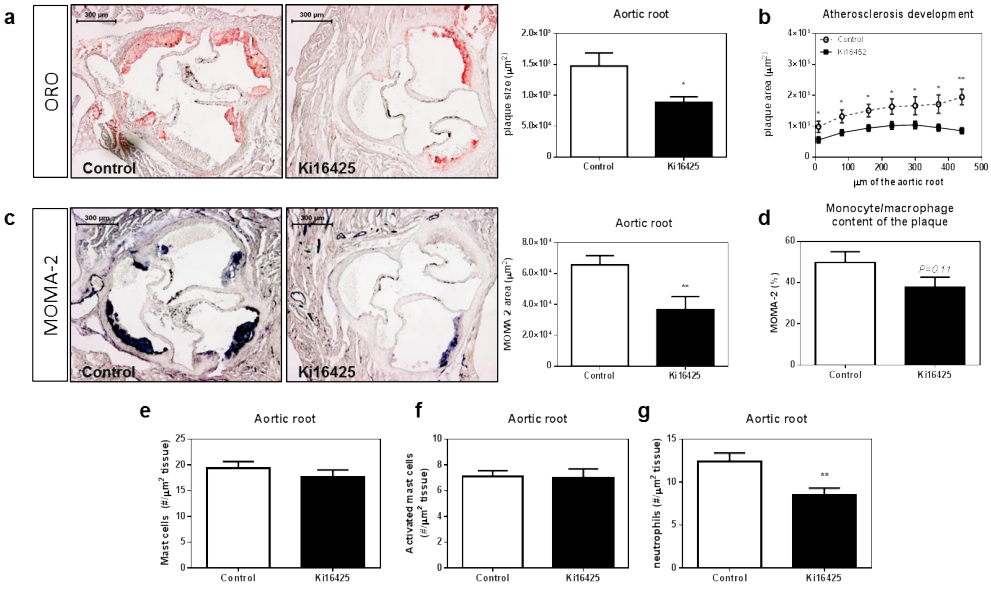

Figure 1: The $LPA_{1/3}$ antagonist, Ki16425, reduces atherosclerosis development. (a) Atherosclerotic plaque size in the aortic root of the heart was determined by an Oil-Red-O staining on 10µm sections; representative pictures are shown. Blockade of receptors $LPA_{1/3}$ resulted in a 40% reduction in atherosclerosis. **(b)** The Ki16425 treated mice had significantly lower atherosclerotic plaque development throughout the entire three valve area of the aortic root. **(c)** Macrophage expression levels were measured using a MOMA-2 staining; $LPA_{1/3}$ antagonism led to 45% less macrophage accumulation within the aortic root of the hearts. **(d)** The relative amount of macrophages in the atherosclerotic plaques was not significantly affected by the Ki16425 treatment.

(e) Mast cell numbers (#) and **(f)** activation state, as well as **(g)** neutrophil numbers were manually quantified using a Naphthol AS-D chloro-acetate esterase staining; no difference was observed in the number or degranulation status of mast cells in the aortic root. Neutrophil numbers were found significantly reduced by 31% in the aortic root of the Ki16425 group as compared to the control. All values (n=12/grp) are depicted as mean±SEM (*P<0.05, **P<0.01).

3.2 Treatment with Ki16425 results in decreased serum total cholesterol levels

$LPA_{1/3}$ inhibition with Ki16425 did not alter body weight (**Figure 2A**) and similarly, analysis of the liver weight or spleen weight at the endpoint of the study presented no change for the treated versus the control group (**Supplementary Figure 1A,B**). Interestingly, total serum cholesterol levels in time upon $LPA_{1/3}$ inhibition, was significantly lower compared to the control group (**Figure 2B**, w3: -20%, P=0.012; w6: -16%, P=0.017). Further analysis of the serum lipoprotein content at the experimental endpoint showed a trend towards decreased LDL levels for the Ki16425 treated mice, as compared to the control (**Figure 2C**, P=0.06).

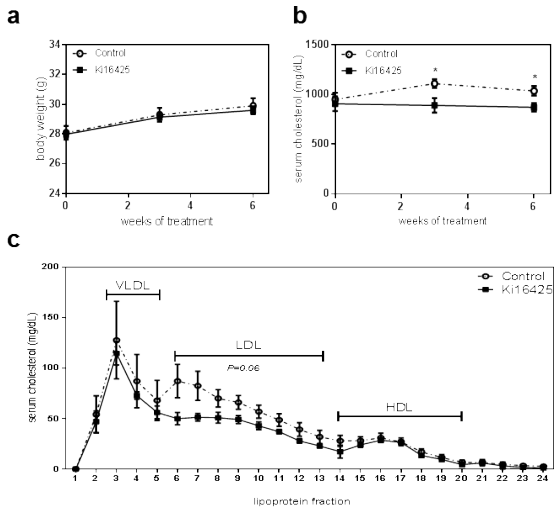

Figure 2: $LPA_{1/3}$ inhibition reduces total cholesterol content in the serum. (a) The animal body weight showed no significant differences throughout 6 weeks of treatment between the groups. **(b)** Total serum cholesterol remained at significantly lower levels in the Ki16425 group compared to the control. **(c)** The Ki16425 treated animals presented a trend towards reduced LDL levels (P=0.06). P-values are calculated by the fraction sum for each lipoprotein per group (n=5/grp). All values are depicted as mean±SEM (*P<0.05).

3.3 Pro-inflammatory CCL2 expression and secretion are reduced upon $LPA_{1/3}$ inhibition

Considering the lower macrophage and neutrophil content of the atherosclerotic plaque, we isolated mRNA from the aortic arch which was subsequently analyzed for the expression levels of different chemokines as well as endothelial adhesion molecules. The expression of ICAM-1, which is tightly linked to LPA[26], did not present any differences between the control and Ki16425 group (**Figure 3A**, P=0.70). The same was observed for

chemokine CXCL1 (**Figure 3B**, P=0.52). The pro-inflammatory chemokine CCL2 showed a trend towards reduction in the aortic arch of the Ki16425 treated mice (**Figure 3C**, P=0.067). Similarly, liver mRNA analysis displayed substantially lower CCL2 expression upon $LPA_{1/3}$ antagonism (**Figure 3D**, P=0.035). In addition, gene expression of the macrophage marker CD68 was significantly reduced in the liver of animals treated with Ki16425 (**Figure 3E**, P=0.037). To establish whether the reduction in CCL2 expression results in diminished protein levels, CCL2 chemokine secretion in the circulation was determined and found considerably lower (-65%) upon $LPA_{1/3}$ inhibition (**Figure 3F**, Ki16425: 58.9±6.4 pg/mL compared to 165.8±32.8 pg/mL, P=0.003).

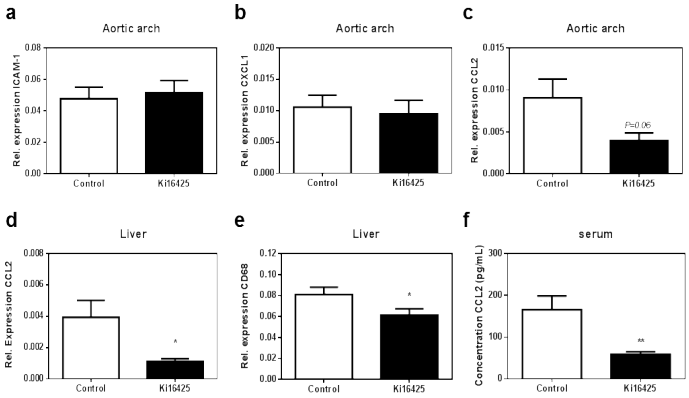

Figure 3: Treatment with Ki16425 decreases CCL2 chemokine expression and release. Gene profiling in the aortic arch displayed no difference between the two groups in **(a)** ICAM-1 or **(b)** CXCL1 chemokine expression levels. **(c)** CCL2 expression showed a slight reduction upon $LPA_{1/3}$ antagonism. **(d)** Liver CCL2 expression was significantly lower in the Ki16425 treated animals compared to the control. **(e)** Macrophage CD68 gene expression in the liver was reduced for the Ki16425 mice compared to the controls. **(f)** CCL2 chemokine secretion was decreased up to 65% in the circulation of the Ki16425 group, compared to the control. Gene expression (n=8/grp) is depicted as relative to two housekeeping genes (β-actin and Rpl27). Serum CCL2 concentration was measured using an ELISA assay (n=13/grp). All values were calculated as mean±SEM. (*P<0.05,**P<0.01).

3.4 $CCR2^+$ neutrophils and monocytes circulate at lower levels upon $LPA_{1/3}$ antagonism

Since the reduced CCL2 levels could lower the inflammatory cell infiltration, and therefore lower the plaque size, it was particularly intriguing to focus on immune cells that respond to this chemokine *via* its specific receptor, CCR2. For that reason, two additional groups of $LDLr^{-/-}$ mice were treated with either Ki16425 or vehicle-control for 6 weeks while on WTD. In the blood the overall percentage of circulating neutrophils, defined as $Ly6G^+CD11b^+/NK1.1^-$ cells, was not affected by the treatment (**Figure**

4A). However, the relative amount of circulating CCR2$^+$ neutrophils was significantly increased over time in the control group (**Figure 4B**, control: w0 compared to w2, P=0.031; w0 compared to w4, P=0.0001), but was found reduced in the treated animals after 4 weeks of $LPA_{1/3}$ inhibition (w4: Ki16425 compared to control, P=0.0060).

Furthermore, the monocyte population in the circulation, defined as Ly6C$^+$/CD11b$^+$Ly6G$^-$/NK1.1$^-$ cells was found to increase in the control group during 4 weeks of treatment (**Figure 4C**, control: w0 compared to w4, P=0.014). At week 4, the Ki16425 treated group showed a trend to reduced monocyte percentage when compared to the control (**Figure 4C**, w4: Ki16425 compared to control, P=0.066). Of this population, the CCR2$^+$ monocytes, which comprise the inflammatory monocyte subset[36] -alternatively defined as Ly6C^{high}- increased greatly in the control group over time (**Figure 4D**, control: w0 compared to w2, P=0.004; w0 compared to w4, P=0.0002), while the CCR2$^+$ monocytes of the treated group were only slightly elevated (Ki16425: w0 compared to w2, P=0.64; w0 compared to w4, P=0.054).

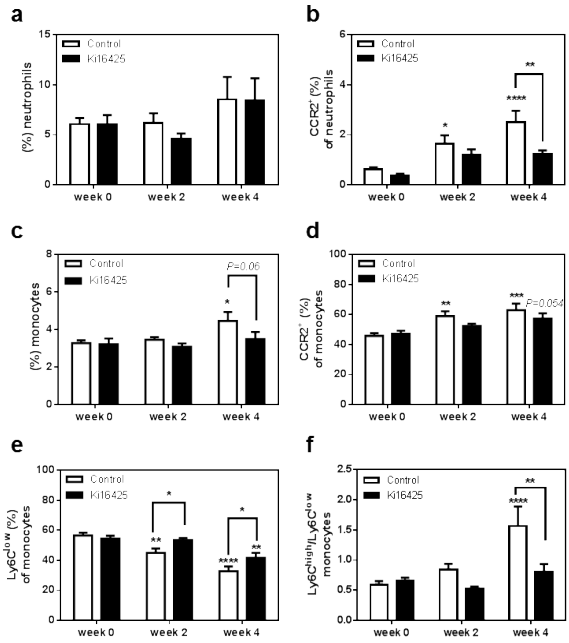

Figure 4: $LPA_{1/3}$ inhibition retains circulating CCR2$^+$ neutrophils and monocytes at low levels while increasing, Ly6C^{low} patrolling monocytes over time. (a) No difference was observed in the circulating neutrophil percentage between the two groups of animals. **(b)** CCR2$^+$ expressing neutrophils were reduced after 4 weeks of $LPA_{1/3}$ antagonism. **(c)** Circulating monocytes showed a slight reduction upon 4 weeks of Ki16425 treatment. **(d)** CCR2$^+$ monocytes remained at lower levels in the course of $LPA_{1/3}$ inhibition. **(e)** Non-inflammatory monocytes appeared significantly higher at 2 and 4 weeks of $LPA_{1/3}$ inhibition. **(f)** The ratio of inflammatory/non-inflammatory monocytes was increased in the control group compared to the treated. All values are calculated as mean±SEM. (n=12/grp, *P<0.05, **P<0.01, ***P<0.001, **** P<0.0001).

On the contrary, Ly6C^{low}-patrolling monocytes of the control mice showed a sharp decline over time (control: w0 compared to w2, P=0.0039; w0 compared to w4, P<0.0001), but upon Ki16425 treatment the decrease was only observed after 4 weeks and was less acute (Ki16425: w0 compared to w4, P=0.0025). Therefore, in relation to the control group, $LPA_{1/3}$ blocked animals presented significantly higher non-inflammatory circulating monocytes over time (**Figure 4E**, Ki16425 compared

to control: w2:P=0.048; w4:P=0.040). Therefore, $LPA_{1/3}$ inhibition retained the inflammatory versus non-inflammatory responses at lower levels as shown by the relative difference of inflammatory versus the non-inflammatory monocytes per group (**Figure 4F**, Ki16425 w4 compared to control w4: P=0.003).

3.5 $LPA_{1/3}$ inhibition increases circulating anti-inflammatory $CD4^+$ T regulatory cells, while decreasing T helper 1 cells

Flow cytometric analysis of the white blood cell population showed a significant reduction in the circulating $CD4^+$ T cell percentage after $LPA_{1/3}$ inhibition (**Figure 5A**, P=0.036). However, within the $CD4^+$ T cell population, anti-inflammatory $FoxP3^+/CD25^+/CD4^+$ T_{REG} percentage was found significantly increased (**Figure 5B**, Ki16425: 10.24 ± 0.71% versus control: 7.06 ± 0.41%, P=0.0013). Among the $CD4^+$ T_{REG} population, $FoxP3^+Helios^-/CD25^+$ cells, defined as inducible (i)T_{REG} and generated in secondary lymphoid organs[37,38], increased significantly in the Ki16425-treated group (**Figure 5C**, P=0.038). The percentage of pro-inflammatory $CD4^+$ T_{H1} cells in the blood was reduced upon $LPA_{1/3}$ inhibition (**Figure 5D**, P=0.011). Also in the spleen, $CD4^+$ T cells were reduced in the Ki16425 treated mice (Fig.5E, P<0.0001), with no difference observed however in the overall $FoxP3^+/CD25^+CD4^+$ T_{REG} population (**Figure 5F**, P=0.39). Nonetheless, $LPA_{1/3}$ inhibition resulted in a significant reduction in the inducible $CD4^+$ T_{REG} cells (**Figure 5G**, P=0.025). No significant differences in T_{H1} cells were observed in this compartment (**Figure 5H**, P=0.09).

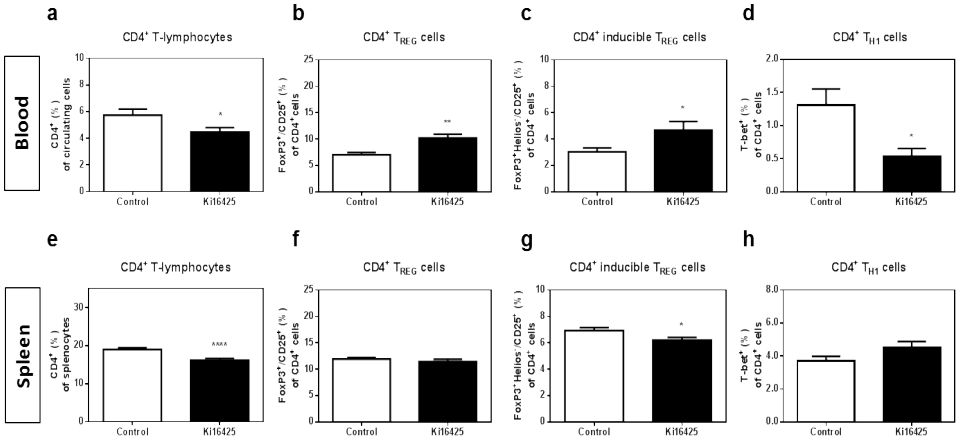

Figure 5: Systemic treatment with Ki16425 for 6 weeks reduces $CD4^+$ T cells in the blood and spleen, with a potency to increase anti-inflammatory T_{REG} cells. (a) Upon 6 weeks of treatment, $LPA_{1/3}$ antagonism reduced the percentage of $CD4^+$ T cells in the blood of $LPA_{1/3}$ blocked mice, as compared to the control. **(b)** Anti-inflammatory $CD4^+$ T_{REG} and **(c)** inducible $FoxP3^+Helios^-$ T_{REG} cells were detected at higher levels in contrast to **(d)** lower inflammatory T_{H1} cells in the blood of the Ki16425 treated mice. **(e)** In the spleen of Ki16425 treated animals $CD4^+$ T cells appeared significantly lower. **(f)** No difference was observed within

the overall $CD4^+$ T_{REG} cells. **(g)** The inducible T_{REG} cells were found substantially decreased. **(h)** No significant difference was detected in the $CD4^+$ T_{H1} population. All values are calculated as mean±SEM. (n=12/grp, *P<0.05,**P<0.01, ****P<0.0001).

In addition, no difference was observed within the $CD8^+$ population present in the blood or spleen of the two groups (**Supplementary Figures 2A,B**). Likewise, MHC-II^+CD11c^{high} dendritic cells (DCs) were not affected by the treatment (**Supplementary Figure 2C**).

3.6 The T cell content of the atherosclerotic plaque is not altered by $LPA_{1/3}$ inhibition

Considering that the systemic differences in the $CD4^+$ T cells upon $LPA_{1/3}$ blockade may directly influence the T cell content inside the atherosclerotic plaque, a $CD3^+$ immunohistochemical staining was performed in the aortic root. However, no significant differences were observed upon manual quantification of the $CD3^+$ cells in the three-valve area of both groups (**Figure 6**, P=0.43).

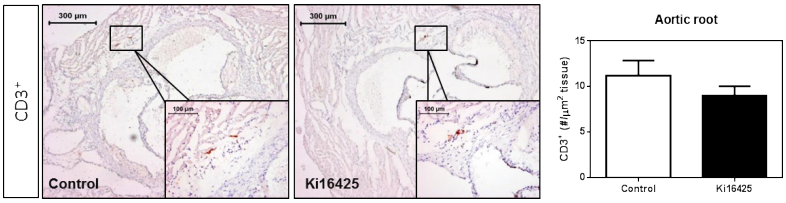

Figure 6: Total $CD3^+$ T cell numbers in the aortic root show no difference between the control and Ki16425-treated groups. $CD3^+$ cells in the aortic root of the hearts were determined upon manual quantification. No difference was observed in the $CD3^+$ expressing cells of the aortic root upon $LPA_{1/3}$ inhibition. All values (n=12/grp) are depicted as mean±SEM.

4. Discussion

In this study we show that pharmacological inhibition of $LPA_{1/3}$ receptors through Ki16425, reduced atherosclerotic plaque development by 40%. Specifically, we have found that $LPA_{1/3}$ antagonism significantly attenuated the macrophage and neutrophil content of the plaque. Furthermore, a mild downregulation of total serum cholesterol was detected, which may have contributed to the decreased atherosclerotic plaque size. We observed a systemic reduction in the expression and secretion of chemokine CCL2, which could have resulted in the detected $CCR2^+$ monocyte and neutrophil decline in the circulation. This decline in $CCR2^+$ cells in the blood seems consistent with the reduction in the absolute amount of macrophages and neutrophils inside the atherosclerotic plaques of the Ki16425 mice. Upon lower levels of circulating

CCL2, less CCR2^{+} monocytes and neutrophils are infiltrating the atherosclerotic site and subsequently there is a reduction in the absolute number of neutrophils and macrophages observed inside the plaque. As the atherosclerotic plaque at this specific timepoint consists primarily of macrophages, the absolute amount actually reflected the reduction in plaque size, whereas the relative macrophage content did not differ. This response is in line with previous evidence supporting that LPA elicits its effects through the release of CCL2 by its target cells[19]. Unlike reports that link the action of LPA to endothelial cell activation[12,26,39], in this investigation we did not observe any differences in the aortic ICAM-1 or CXCL1 expression levels. It is important to mention however that in a previously published study by Zhou et al., the atherosclerotic effects of LPA were mainly associated with endothelial activation through chemokine CXCL1[25] and not with the CCL2-CCR2 axis. Furthermore, in their study no effect was observed on cholesterol metabolism, whereas we detected a reduction in LDL cholesterol levels. Considering that the above experiments were performed in apoE$^{-/-}$ mice, it is possible that strain specific effects are responsible for the different mechanism observed[40]. In the past, numerous studies have examined the differences between the LDLr$^{-/-}$ and apoE$^{-/-}$ models. The leading distinction between the two strains is that LDLr$^{-/-}$ mice do not develop atherosclerosis unless placed on a high-cholesterol diet[41], whereas apoE$^{-/-}$ mice have basal plaque formation even on chow diet[42]. Thereupon, apoE$^{-/-}$ mice develop higher plasma cholesterol levels and more pronounced plaques upon WTD, while showing lower plaque T cell numbers[43]. In addition, apoE$^{-/-}$ mice, unlike the LDLr$^{-/-}$, exhibit impaired formation and efflux of HDL particles, an effect which is highly distinct from the human case[44]. With the above in mind, we considered LDLr$^{-/-}$ as a model that does not show atherosclerosis-related systemic effects prior to WTD. It is important to mention that the presence of apoE can affect monocyte formation and accumulation in the plaque[45], which could account for the main difference between the two models in regard to the role of $LPA_{1/3}$ receptors. In addition, apoE$^{-/-}$ and LDLr$^{-/-}$ mice have also proven to differ in the ABCA1-mediated cholesterol transportation pathway[46,47]. This may explain the reason why LDLr$^{-/-}$ mice show differences in cholesterol regulation upon $LPA_{1/3}$ inhibition, an effect which was absent in apoE$^{-/-}$ mice. Nevertheless, in both experimental sets $LPA_{1/3}$ inhibition substantially reduced plaque development to a similar extend despite the fact that the apoE$^{-/-}$ mice were treated with Ki16425 daily for 3 months while in our study LDLr$^{-/-}$ mice were injected 3x/week for a 6 week period.

Furthermore, in our study, the patrolling Ly6C^{low} population was increased already after two weeks of Ki16425 treatment, suggesting an additional anti-inflammatory effect. This anti-inflammatory subtype of mouse monocytes expressing the Ly6C protein at low levels, has been previously reported to play a crucial role in the control of atherosclerosis development since LDLr$^{-/-}$ mice that lack this subtype showed increased plaque formation[48]. Therefore, the anti-inflammatory effects of patrolling

monocytes detected upon $LPA_{1/3}$ antagonism may have contributed to the reduction in atherosclerosis development. Together, it seems that Ki16425 carries out its effects primarily by regulating the immune response, since also the $CCR2^+$ monocytes and neutrophils are circulating at lower levels compared to the control, already at the second week of treatment. This does not exclude the fact that cholesterol lowering mechanisms may have been partly responsible for the reduced disease progression.

In the past, LPA has also been reported to affect the proliferation of T lymphocytes[49]. Here we observe that upon $LPA_{1/3}$ antagonism, $CD4^+$ T cells are substantially diminished, which may have been due to a reduction in LPA induced mitogenesis[18]. Furthermore, LPA can promote the migration of $CD4^+$ T cells[33], but not of $CD8^+$ T cells[50]. This is in line with our observations on $CD4^+$ T cells being markedly reduced upon $LPA_{1/3}$ inhibition, while no effects were detectable on the $CD8^+$ T cell population in either the blood or spleen. Similarly, no differences were found in the dendritic cell population; however, the effects of LPA on DCs seem to depend on their state. For example, mouse DCs were previously reported to migrate towards LPA upon LPA_3 activation, yet for that to take place they had to be in an immature state[51]. As mentioned above, $CD4^+$ T cells can migrate in response to LPA, but this action was previously shown to depend on the expression of LPA_1 and LPA_2. Specifically, these two receptors are considered to have an inverse impact on T cell migration, with LPA_1 enhancing it while LPA_2 hinders it, depending though also on whether the cells are in a naive or activated state[50]. This fact further illustrates the complexity behind LPA signaling and how different receptor signaling pathways can have entirely opposing actions.

Notably, while $CD4^+$ T cell levels were reduced upon Ki16425 treatment, the anti-inflammatory T_{REG} cells were strongly enhanced. To our knowledge, there is thus far no evidence describing the relationship between $LPA_{1/3}$ inhibition and T_{REG} induction. The observed effects indicate that $LPA_{1/3}$ inhibition can skew the adaptive immune system towards an anti-inflammatory response as demonstrated by the overall lower $CD4^+$ levels, with the pro-inflammatory T_{H1} subset found relatively decreased in the blood while the athero-protective[52] $CD4^+$ T_{REG} cells were circulating at increased levels.

However, the differences on the $CD4^+$ population in the blood and spleen did not reflect the T cell numbers inside the plaques of the treated mice. This suggests that the reduced atherosclerotic plaque size observed upon $LPA_{1/3}$ antagonism was not mediated through a difference in local T cell responses, but was rather elicited *via* a systemic anti-inflammatory effect of the Ki16425 treatment. Moreover, we found no difference on the mast cell counts in the atherosclerotic plaques of the treated mice, despite previous evidence that mast cells respond to LPA through $LPA_{1/3}$ receptors[53]. Recent studies have also implicated additional LPA receptors present on the mast cell surface, which may induce mast cell activation in an $LPA_{1/3}$ independent fashion[54]. Furthermore, mast cell

effects mediated by LPA could also depend on the state of atherosclerosis. For instance, our group has previously reported that mast cell activation through LPA leads to advanced plaque destabilization[19], while in this study we aimed our attention in early plaque development.

In conclusion, $LPA_{1/3}$ receptor inhibition through Ki16425 induced systemic anti-inflammatory responses *via* a reduction in CCL2-CCR2 signaling, an enhancement of anti-inflammatory innate, as well as adaptive, immune responses and a decrease in plasma cholesterol levels, collectively resulting in the reduction of the atherosclerotic burden. The anti-inflammatory immune reaction of Ki16425 may span even outside atherosclerosis and into other diseases, which are characterized by excessive inflammation. For instance, Ki16425 has been found to reduce inflammation in experimental models for obesity[55], rheumatoid arthritis[56], and lung fibrosis[57]. Thus, the importance of singularly targeting the $LPA_{1/3}$ receptors *via* pharmacological inhibition may grant anti-inflammatory effects without completely shutting down the immune response. At the same time it retains possible positive effects that LPA may evoke through its additional receptors in other physiological processes inside the body. Therefore, $LPA_{1/3}$ inhibition is an interesting therapy with multiple beneficial effects that can be employed in a broad spectrum of diseases, among which atherosclerosis.

Reference list:

1. Mozaffarian, D. *et al.* Heart Disease and Stroke Statistics-2016 Update: A Report From the American Heart Association. *Circulation* **133,** e38–e360 (2016).
2. Libby, P., Ridker, P. M. & Hansson, G. K. Progress and challenges in translating the biology of atherosclerosis. *Nature* **473,** 317–25 (2011).
3. Libby, P., Lichtman, A. H. & Hansson, G. K. Immune effector mechanisms implicated in atherosclerosis: from mice to humans. *Immunity* **38,** 1092–1104 (2013).
4. Drechsler, M., Megens, R. T. A., van Zandvoort, M., Weber, C. & Soehnlein, O. Hyperlipidemia-triggered neutrophilia promotes early atherosclerosis. *Circulation* **122,** 1837–1845 (2010).
5. Bot, I. *et al.* Mast cell chymase inhibition reduces atherosclerotic plaque progression and improves plaque stability in ApoE-/- mice. *Cardiovasc. Res.* **89,** 244–252 (2011).
6. Zernecke, A. Dendritic cells in atherosclerosis: evidence in mice and humans. *Arterioscler. Thromb. Vasc. Biol.* **35,** 763–770 (2015).
7. Frostegard, J. *et al.* Cytokine expression in advanced human atherosclerotic plaques: dominance of pro-inflammatory (Th1) and macrophage-stimulating cytokines. *Atherosclerosis* **145,** 33–43 (1999).
8. Dohi, T. *et al.* Increased circulating plasma lysophosphatidic acid in patients with acute coronary syndrome. *Clin. Chim. Acta.* **413,** 207–212 (2012).
9. Tokumura, A. *et al.* Increased formation of lysophosphatidic acids by lysophospholipase D in serum of hypercholesterolemic rabbits. *J. Lipid Res.* **43,** 307–315 (2002).
10. Yao, C.-S. *et al.* Patients with risk factors have higher plasma levels of lysophosphatidic acid: a promising surrogate marker for blood platelet activation. *Blood Coagul. Fibrinolysis* **25,** 322–325 (2014).
11. Eichholtz, T., Jalink, K., Fahrenfort, I. & Moolenaar, W. H. The bioactive phospholipid lysophosphatidic acid is released from activated platelets. *Biochem. J.* **291 (Pt 3,** 677–680 (1993).
12. Siess, W. *et al.* Lysophosphatidic acid mediates the rapid activation of platelets and endothelial cells by mildly oxidized low density lipoprotein and accumulates in human atherosclerotic lesions. *Proc. Natl. Acad. Sci. U. S. A.* **96,** 6931–6936 (1999).
13. Bot, M. *et al.* Atherosclerotic lesion progression changes lysophosphatidic acid homeostasis to favor its accumulation. *Am. J. Pathol.* **176,** 3073–3084 (2010).
14. Siess, W. Platelet interaction with bioactive lipids formed by mild oxidation of low-density lipoprotein. *Pathophysiol. Haemost. Thromb.* **35,** 292–304 (2006).
15. Chun, J., Hla, T., Lynch, K. R., Spiegel, S. & Moolenaar, W. H. International Union of Basic and Clinical Pharmacology. LXXVIII. Lysophospholipid receptor nomenclature. *Pharmacol. Rev.* **62,** 579–587 (2010).
16. Choi, J. W. *et al.* LPA receptors: subtypes and biological actions. *Annu. Rev. Pharmacol. Toxicol.* **50,** 157–186 (2010).
17. Fukushima, N. & Chun, J. The LPA receptors. *Prostaglandins Other Lipid Mediat.* **64,** 21–32 (2001).
18. Yung, Y. C., Stoddard, N. C. & Chun, J. LPA receptor signaling: pharmacology, physiology, and pathophysiology. *J. Lipid Res.* **55,** 1192–1214 (2014).
19. Bot, M. *et al.* Lysophosphatidic acid triggers mast cell-driven atherosclerotic plaque destabilization by increasing vascular inflammation. *J. Lipid Res.* **54,** 1265–1274 (2013).
20. Hashimoto, T., Ohata, H. & Honda, K. Lysophosphatidic acid (LPA) induces plasma exudation and histamine release in mice via LPA receptors. *J. Pharmacol. Sci.* **100,** 82–87 (2006).

21. Hashimoto, T., Yamashita, M., Ohata, H. & Momose, K. Lysophosphatidic acid enhances in vivo infiltration and activation of guinea pig eosinophils and neutrophils via a Rho/Rho-associated protein kinase-mediated pathway. *J. Pharmacol. Sci.* **91,** 8–14 (2003).
22. Wang, L., Knudsen, E., Jin, Y., Gessani, S. & Maghazachi, A. A. Lysophospholipids and chemokines activate distinct signal transduction pathways in T helper 1 and T helper 2 cells. *Cell. Signal.* **16,** 991–1000 (2004).
23. Schober, A. & Siess, W. Lysophosphatidic acid in atherosclerotic diseases. *Br. J. Pharmacol.* **167,** 465–82 (2012).
24. Lin, C. I., Chen, C.-N., Chen, J. H. & Lee, H. Lysophospholipids increase IL-8 and MCP-1 expressions in human umbilical cord vein endothelial cells through an IL-1-dependent mechanism. *J. Cell. Biochem.* **99,** 1216–1232 (2006).
25. Zhou, Z. *et al.* Lipoprotein-derived lysophosphatidic acid promotes atherosclerosis by releasing CXCL1 from the endothelium. *Cell Metab.* **13,** 592–600 (2011).
26. Lee, H. *et al.* Lysophospholipids increase ICAM-1 expression in HUVEC through a Gi- and NF-kappaB-dependent mechanism. *Am. J. Physiol. Cell Physiol.* **287,** C1657–66 (2004).
27. Zhou, Z. *et al.* Lipoprotein-derived lysophosphatidic acid promotes atherosclerosis by releasing CXCL1 from the endothelium. *Cell Metab.* **13,** 592–600 (2011).
28. Goetzl, E. J., Kong, Y. & Voice, J. K. Cutting edge: differential constitutive expression of functional receptors for lysophosphatidic acid by human blood lymphocytes. *J. Immunol.* **164,** 4996–4999 (2000).
29. Li, S., Xiong, C. & Zhang, J. ATX and LPA receptor 3 are coordinately up-regulated in lipopolysaccharide-stimulated THP-1 cells through PKR and SPK1-mediated pathways. *FEBS Lett.* **586,** 792–797 (2012).
30. Chou, C.-H. *et al.* Lysophosphatidic acid alters the expression profiles of angiogenic factors, cytokines, and chemokines in mouse liver sinusoidal endothelial cells. *PLoS One* **10,** e0122060 (2015).
31. Damirin, A. *et al.* Role of lipoprotein-associated lysophospholipids in migratory activity of coronary artery smooth muscle cells. *Am. J. Physiol. Heart Circ. Physiol.* **292,** H2513–22 (2007).
32. Chan, L. C. *et al.* LPA3 receptor mediates chemotaxis of immature murine dendritic cells to unsaturated lysophosphatidic acid (LPA). *J. Leukoc. Biol.* **82,** 1193–1200 (2007).
33. Tanikawa, T., Kurohane, K. & Imai, Y. Regulatory effect of lysophosphatidic acid on lymphocyte migration. *Biol. Pharm. Bull.* **33,** 204–208 (2010).
34. Brault, S. *et al.* Lysophosphatidic acid induces endothelial cell death by modulating the redox environment. *Am. J. Physiol. Regul. Integr. Comp. Physiol.* **292,** R1174–83 (2007).
35. Ohta, H. *et al.* Ki16425, a subtype-selective antagonist for EDG-family lysophosphatidic acid receptors. *Mol. Pharmacol.* **64,** 994–1005 (2003).
36. Serbina, N. V & Pamer, E. G. Monocyte emigration from bone marrow during bacterial infection requires signals mediated by chemokine receptor CCR2. *Nat. Immunol.* **7,** 311–317 (2006).
37. Thornton, A. M. *et al.* Expression of Helios, an Ikaros transcription factor family member, differentiates thymic-derived from peripherally induced Foxp3+ T regulatory cells. *J. Immunol.* **184,** 3433–3441 (2010).
38. Akimova, T., Beier, U. H., Wang, L., Levine, M. H. & Hancock, W. W. Helios expression is a marker of T cell activation and proliferation. *PLoS One* **6,** e24226 (2011).
39. Rizza, C. *et al.* Lysophosphatidic acid as a regulator of endothelial/leukocyte interaction. *Lab. Invest.* **79,** 1227–1235 (1999).
40. Getz, G. S. & Reardon, C. A. Do the Apoe-/- and Ldlr-/- Mice Yield the Same Insight on Atherogenesis? *Arteriosclerosis, thrombosis, and vascular biology* (2016). doi:10.1161/ATVBAHA.116.306874

41. Zhang, S. H., Reddick, R. L., Piedrahita, J. A. & Maeda, N. Spontaneous hypercholesterolemia and arterial lesions in mice lacking apolipoprotein E. *Science* **258,** 468–471 (1992).

42. Ishibashi, S., Goldstein, J. L., Brown, M. S., Herz, J. & Burns, D. K. Massive xanthomatosis and atherosclerosis in cholesterol-fed low density lipoprotein receptor-negative mice. *J. Clin. Invest.* **93,** 1885–1893 (1994).

43. Roselaar, S. E., Kakkanathu, P. X. & Daugherty, A. Lymphocyte populations in atherosclerotic lesions of apoE -/- and LDL receptor -/- mice. Decreasing density with disease progression. *Arterioscler. Thromb. Vasc. Biol.* **16,** 1013–1018 (1996).

44. Tani, M. *et al.* The influence of apoE-deficiency and LDL-receptor-deficiency on the HDL subpopulation profile in mice and in humans. *Atherosclerosis* **233,** 39–44 (2014).

45. Murphy, A. J. *et al.* ApoE regulates hematopoietic stem cell proliferation, monocytosis, and monocyte accumulation in atherosclerotic lesions in mice. *J. Clin. Invest.* **121,** 4138–4149 (2011).

46. Bi, X. *et al.* Myeloid cell-specific ATP-binding cassette transporter A1 deletion has minimal impact on atherogenesis in atherogenic diet-fed low-density lipoprotein receptor knockout mice. *Arterioscler. Thromb. Vasc. Biol.* **34,** 1888–1899 (2014).

47. Joyce, C. W. *et al.* The ATP binding cassette transporter A1 (ABCA1) modulates the development of aortic atherosclerosis in C57BL/6 and apoE-knockout mice. *Proc. Natl. Acad. Sci. U. S. A.* **99,** 407–412 (2002).

48. Hanna, R. N. *et al.* NR4A1 (Nur77) deletion polarizes macrophages toward an inflammatory phenotype and increases atherosclerosis. *Circ. Res.* **110,** 416–427 (2012).

49. Goetzl, E. J., Kong, Y. & Mei, B. Lysophosphatidic acid and sphingosine 1-phosphate protection of T cells from apoptosis in association with suppression of Bax. *J. Immunol.* **162,** 2049–2056 (1999).

50. Zheng, Y., Voice, J. K., Kong, Y. & Goetzl, E. J. Altered expression and functional profile of lysophosphatidic acid receptors in mitogen-activated human blood T lymphocytes. *FASEB J. Off. Publ. Fed. Am. Soc. Exp. Biol.* **14,** 2387–2389 (2000).

51. Chan, L. C. *et al.* LPA3 receptor mediates chemotaxis of immature murine dendritic cells to unsaturated lysophosphatidic acid (LPA). *J. Leukoc. Biol.* **82,** 1193–200 (2007).

52. Klingenberg, R. *et al.* Depletion of FOXP3+ regulatory T cells promotes hypercholesterolemia and atherosclerosis. *J. Clin. Invest.* **123,** 1323–1334 (2013).

53. Bagga, S. *et al.* Lysophosphatidic acid accelerates the development of human mast cells. *Blood* **104,** 4080–7 (2004).

54. Lundequist, A. & Boyce, J. A. LPA5 is abundantly expressed by human mast cells and important for lysophosphatidic acid induced MIP-1beta release. *PLoS One* **6,** e18192 (2011).

55. Rancoule, C. *et al.* Lysophosphatidic acid impairs glucose homeostasis and inhibits insulin secretion in high-fat diet obese mice. *Diabetologia* **56,** 1394–402 (2013).

56. Orosa, B. *et al.* Lysophosphatidic acid receptor inhibition as a new multipronged treatment for rheumatoid arthritis. *Ann. Rheum. Dis.* **73,** 298–305 (2014).

57. Tager, A. M. *et al.* The lysophosphatidic acid receptor LPA1 links pulmonary fibrosis to lung injury by mediating fibroblast recruitment and vascular leak. *Nat. Med.* **14,** 45–54 (2008).

58. Chomczynski, P. & Sacchi, N. The single-step method of RNA isolation by acid guanidinium thiocyanate-phenol-chloroform extraction: twenty-something years on. *Nat. Protoc.* **1,** 581–585 (2006).

Supplementary Information

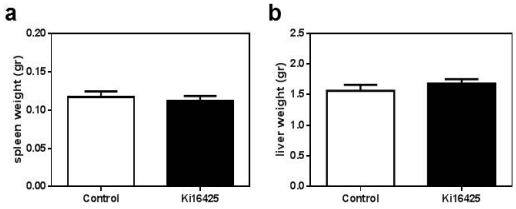

Figure 1: Treatment with Ki16425 does not affect the spleen or liver weight of mice. (a) The spleen weight between the control and Ki16425 treated group showed no significant difference (P=0.63) at the end of the study. **(b)** Similarly, the liver weight between the control and Ki16425 groups was not substantially different (P=0.38). All values (n=13/grp; spleen and n=6/grp; liver) are depicted as mean±SEM.

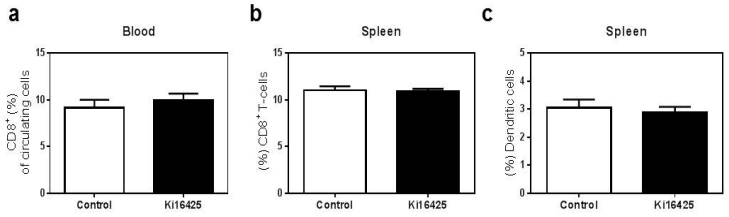

Figure 2: $LPA_{1/3}$ inhibition did not affect the amount of $CD8^+$ T lymphocytes or dendritic cells. The amount of $CD8^+$ T cells in the **(a)** circulation and **(b)** spleen was not affected by treatment with Ki16425 (P=0.50) and (P=0.78). **(c)** The overall percentage of dendritic cells present in the spleen showed no differences among the control and treated mice (P=0.60). All values (n=12/grp) are depicted as mean±SEM.

Gene	*Forward primer (5'-3')*	*Reverse primer (3'-5')*
CCL2	GCATCT GCCCTAAGGTCT TCA	TTCACTGTCACACTGGTCACTCCTA
CD68	TGCCTGACAAGGGACACTTCGGG	GCGGGTGATGCAGAAGGCGATG
CXCL1	TTGACCCTGAAGCTCCCTTG	AGGTGCCATCAGAGCAGTC
I-CAM 1	GTCCGCTTCCGCTACCATCA	GGTCCTTGCCTACTTGCTGCC
Rpl27	CGCCAAGCGATCCAAGATCAAGTCC	AGCTGGGTCCCTGAACACATCCTTG
β-actin	AACCGTGAAAAGATGACCCAGAT	CACAGCCTGGATGGCTACGTA

Supplementary Table 1: qPCR gene primer sequences. All gene expression analysis was performed using two housekeeping genes (β-actin and Rpl27). Abbreviations: Chemokine C-C motif ligand 2 (CCL2); cluster of differentiation 68 (CD68); chemokine C-X-C motif ligand 1 (CXCL1); Intercellular adhesion molecule-1 (ICAM-1); 60s ribosomal protein ligand 27 (Rpl27).

Antibody	Fluorochrome	Clone	Company
CD11b	eFluor 450	M1/70	Ebioscience
Ly6C	PercP Cy5.5	HK1.4	Ebioscience
Ly6G	PE	1A8	BD Biosciences
CCR2	APC	#475301	R&D Systems
CD4	PercP	Rm4-5	BD Biosciences
CD25	FITC	PC61.5	Ebioscience
NK1.1	FITC	PK136	Ebioscience
CD8a	PercP	53-6.7	BD Biosciences
MHC-II	eFluor 450	AF6-120.1	Ebioscience
CD11c	APC	N418	Ebioscience
FoxP3	*eFluor 450*	*FJK-16s*	Ebioscience
T-bet	*Alexa -Fluor 660*	*eBio4B10*	Ebioscience
Helios	*Alexa-Fluor 647*	*22F6*	Ebioscience

Supplementary Table 2: List of extracellular and *intracellular* antibodies used.